nature electronics

Article

https://doi.org/10.1038/s41928-023-01069-w

Brain organoid reservoir computing for artificial intelligence

In the format provided by the authors and unedited

Table-of-contents

Materials and Methods

Human stem cell culture. Human embryonic stem cell line (WA09) was obtained from WiCell institute. The cells were handled under the guidelines of both WiCell Institute and Indiana University Biosafety Committee. WA09 cells were cultured on Growth Factor Reduced Matrigel (Corning) coated 6-well plates with mTESR plus medium (Stemcell Technologies) in a humidified incubator at 37ºC and 5% CO_2. Medium was changed every other day. WA09 cells were passaged every 5 days using ReLeSR (Stemcell Technologies).

Generation of human cortical organoids. Human cortical organoids were generated from human embryonic stem cells (WA09). Embryonic bodies (EBs) were fabricated using a 96-well U bottom microplate (Corning) by aggregation of ~9,000 WA09 cells per well, and then cultured in 100 µL mTESR plus medium (Stemcell Technologies) supplemented with 10 µM SB431542 (SB; Stemgent),1 µM Dorsomorphin (Dorso; R&D Systems) and 10 µM Y-27632 (SelleckChem). After the EB formation (Day 1), the EBs were switched to mTESR plus medium containing 10 µM SB and 1 µM Dorso. After 3-days culture, the cultures were then transferred to cortical organoid medium I (CoM I) [Neurobasal (Life Technologies) supplemented with GlutaMAX, 1% Gem21 NeuroPlex (Gemini Bio-Products), 1% N2 NeuroPlex (Gemini Bio-Products), 1% NEAA (Life Technologies), 1% P/S (Life Technologies), 10 µM SB and 1 µM Dorso] for the next 7 days. On day 10, the cultures were transferred to cortical organoid medium II (CoM II) [Neurobasal with GlutaMAX, 1% Gem21 NeuroPlex, 1% NEAA and 1% P/S] supplemented with 20 ng/mL FGF2 (Life Technologies) for 7 days, followed by 7 additional days in CoM II supplemented with 20 ng/mL of FGF2 and 20 ng/mL EGF (PeproTech, Rocky Hill, NJ, USA). Next, the cultures were transferred to cortical organoid medium III (CoM III) [CoM II supplemented with 10 ng/mL of BDNF, 10 ng/mL of GDNF, 10 ng/mL of NT-3 (all from PeproTech), 200 µM L-ascorbic acid and 100 µM cAMP (Sigma-Aldrich) to promote maturation, gliogenesis and activity]. After 7 days, the assembled cortical organoids were maintained in CoM II supplied with 0.2 ng/mL BDNF, 0.2 ng/mL GDNF, 0.2 ng/mL NT-3, and 1 µM cAMP. Medium change was performed every other day during this process except when specified. From day 30 on, the organoid cultures were transferred to individual wells in a 24 well plate and kept on an orbital shaker at 60 rpm. Detailed medium composition is listed in **Supplementary Table 2.**

Cryo-section and immunostaining of organoids. The organoids were washed three times in 1x Phosphate-Buffered Saline (PBS, Gibco) and then fixed in 4% paraformaldehyde (PFA) in 1x PBS (Thermo Scientific) overnight at 4ºC. The organoids were rinsed three times with 1x PBS and then transferred into 30% sucrose (w/v) solution overnight at 4 ºC for cryoprotection. The organoids were then incubated with 7.5% gelatin (w/v) and 10% sucrose (w/v) in PBS solution at 37 ºC for 1 hour. Finally, the organoids were snap-frozen onto a cryomold (Sakura Finetek) in a dry ice/ethanol slurry. The frozen samples were then sectioned at 30 µm thickness on a cryostat (Leica). To characterize the cultured cortical organoids, the sectioned organoid samples were placed onto charged glass slides and washed three times with 1x PBS. The sectioned samples were then treated with 3N hydrochloric acid (HCl) for 15 minutes for antigen retrieval. Following HCl treatment, the sectioned samples were washed again twice with 1x PBS and subjected to blocking (0.3% Triton-X100, 5% normal goat serum in 1x PBS) for 1 hour, followed by primary

antibody incubation in a humidified chamber at 4 ºC overnight. The sectioned samples were then washed 3 times with 1x PBS followed by secondary antibody incubation at room temperature for 1 hour before being washed and cover slipped with ProLong Gold Antifade Mounting medium containing DAPI (Invitrogen). Detailed antibody information and dilution factors can be found in **Supplementary Table. 3**.

Whole mount staining of organoids. The organoids were first washed three times in 1x PBS and then fixed in 4% PFA in PBS for 1 hour. The fixed organoids were then washed three times with 1x PBS and subjected to blocking (0.5 % Triton-X100, 0.5 % Tween 20, 1 % BSA, 3 % FBS, and 1% of 1% (wt/vol) sodium deoxycholate solution in 1x PBS) for 2 hours in room temperature. Followed by primary antibody incubation in blocking solution with on a gentle rocker at 4 ºC for 2 days, the organoids were then washed 5 times with 1x PBS followed by secondary antibody incubation at 4 ºC for 2 days before being washed with 1x PBS and dehydrated with serial Ethanol solutions (50%, 70%, 100%, 100%) for 2 hours each. The dehydrated organoids were dried and transferred to Benzyl Alcohol/ Benzyl Benzoate (BABB) clearing solution (2 parts benzyl benzoate, 1 part benzyl alcohol). The organoids were incubated until becoming transparent and were imaged under a confocal microscope (Olympus OSR spinning disk) with a 20x objective.

Plating organoids on MEA. After 2 months culture, the organoids were plated into the MaxOne Multielectrode arrays (MEA; Maxwell Biosystems, AG, Switzerland). This multielectrode array (MEA) system allows high-resolution electrophysiological measurement of organoids using meta-oxide-semiconductor (CMOS) technology and allows the recording of up to 1024 channels and stimulation of up to 32 electrodes simultaneously. The MEA chips were first coated with 0.07% polyethylenimine (PEI) for 1 hr and then coated with 5 µg/ml human 521 Laminin for 30 minutes to facilitate organoid adhesion. The organoids plated in MEA system were first cultured in BrainPhys medium (Stemcell technology) with 2% NeuroCult™ SM1 neuronal supplement (Stemcell technology) and 1% P/S (Life Technologies)) supplied with 10ng/mL BDNF and 0.5 µg/ml laminin to promote organoid adhesion. Then the organoids were maintained in BrainPhys medium in a humidified incubator at 37 ºC and 5 % CO_2. A 50% media change was performed every day. Seven days after plating the organoids were ready for recording and stimulation. The experiments were performed 4-6 hours after medium change.

Electrical stimulation. The organoids were stimulated with multiple bipolar voltage pulses via the MEA system. The stimulation electrodes were selected based on the largest spike voltage in the activity scan (the minimum distance between stimulation electrodes was 100 µm) to ensure optimal stimulation efficiency. By applying bipolar electrical pulses with different parameters (pulse voltage = 100 ~ 1000 mV, pulse time = 100~500 µs, pulse interval = 50 ~ 400 ms), the responding neural activity of the organoid was recorded and analyzed. The average mean firing rate of the top-32 most active electrodes in the 200 ms time window after stimulation was calculated for determining non-linear dynamics and fading memory. For the computing tasks, the electrical stimulation was delivered at a given frequency, voltage and interval as encoded with different input information to the stimulation electrodes.

Neural activity measurement. Licensed MaxLab Live Scope V20.1 software was used to run activity scans. Checkerboard assays consisting of 14 configurations at 60 seconds of spike-only record time were run daily to access the area with the active electrical activity of cortical organoids. The gain was set to 512x with a 300 Hz high pass filter. The spike threshold was set to be a signal 5.5 sigma greater than background noise as per recommended software settings. An electrical activity map of an organoid with spike amplitude and rate could be obtained by the MaxLab Live software. (**Supplementary Fig. 3**) Based on the assay results, 1024 electrodes (limited by MEA hardware) with active electrical activity were selected for further spontaneous recordings and performing computing tasks.

Spike sorting. As the electrode size (12.5 μm) of the MaxOne MEA chip is smaller than the expansion area of a single neuron, multiple electrodes may sense the electrical signal from the same neuron. Spike sorting is needed to extract single-unit activity from the raw MEA recordings. The raw traces were band-pass filtered between 300-6000 Hz before applying the Kilosort2 algorithm[1]. The spike sorting output was automatically curated by removing units with an ISI violation threshold above 0.3, an average firing rate below 0.05 Hz, and a signal to noise ratio (SNR) below 5. The filtered traces in time were concatenated before applying spike sorting to process data from the same chip with the same electrode configuration, recorded within a short period of time. All the processing was performed using the SpikeInterface framework[2].

Spike time tiling coefficient to draw a functional connectivity map. The functional connectivity was calculated by recording the spontaneous neuronal activity of organoids. Correlation of neural activity spike trains from each channel was evaluated using spike time tiling coefficient (STTC)[3]. STTC measures synchrony in a spike rate independent manner, distinguishing it from traditional correlation analysis.[3] A publicly available python function (Elephant[4]) was used to compute the STTC. The correlation time window (Δt) was set to 20 ms to compute the functional connectivity weights of all channels. The correlation matrix was further threshold at 0.35 for further analysis (the threshold was chosen to rule out most random connectivity)[5]. A customized python script was developed to draw the functional connectivity map based on the calculated correlation weights of all channels, the nodes and connections were drawn corresponding to the physical location of the electrodes.

Implementing the reservoir computing task of speech recognition. The audio clips were first preprocessed using Mel-frequency cepstral coefficients (MFCCs)[6]. MFCCs are widely used in speech recognition, and a MFCC represents sound clips as a short-term power spectrum, which performs a linear cosine transform of a log power spectrum on a nonlinear Mel-frequency. Mel-frequency bands are equally spaced on the Mel scale, which mimics the frequency response of human auditory systems.[7] In our case, the sound clips were transformed into a set of 12-dimensional vectors (corresponding to the Mel-frequency band channels) with up to 29-time steps. One example representing vowel ‘a’ by speaker 1 is shown in **Supplementary Fig. 8a**. The raw audio clip was preprocessed to MFCCs with 12 frequency channels (y-axis) along time steps (x-axis), each data point on the graph represents the firing probability of an input channel corresponding to a specific frequency band at a specific time point. Such MFCC matrix was then digitized to form stimulation pulses streaming inputs to the organoid through the 12 stimulation

electrodes (selected as described in the 'Electrical Stimulation Session'). The digitized stimulation streams were used to stimulate brain organoids at 100 ms intervals for each time step mixed with latency encoding, which delayed stimulation by the summed power of the current time step to a maximum of 50 ms. The evoked electrical activity was recorded, and the spikes were detected and binned into 10ms time bins with the logistic regression decoding algorithms to obtain the final classification output.

Implementing the reservoir computing task of predicting Hénon map equation. The Hénon map equation was implemented following a similar workflow. The Xn value was first normalized by the min-max range of the whole dataset, then converted into a 1D decomposition of 12 channels (binary 12 bits barcode). The 12 bits barcode was then converted to stimulation pulses of 12 stimulation electrodes (1: stimulation on, 0: no stimulation), and the spatial stimulation representing Hénon map Xn value was input to organoids at 100 ms intervals, and stimulation was delayed by the value of current time step to maximum of 50ms on top of a fixed 100ms interval.

Temporal-spatial sequence encoding strategy. Different encoding strategies (e.g., place-coded, latency-coded, and multiplex index-coded strategy) were tested, as shown in **Supplementary Fig. 10**. Place coding means the input information was represented by the on or off status of stimulation pulses of the stimulation electrode channels, while the stimulation was given at a fixed interval. Latency coding indicates the input information was represented by the latency of each stimulation pulses to a fixed time clock, while all the stimulation channels were on or off simultaneously. Multiplex index coding combines the above two strategies together, both the on and off status of stimulation channels and stimulation latency represents input information.

Read-out function. The evoked spiking activity was extracted from raw recordings as previously described. The spiking activity from the top active electrodes (the different decoding setting was tested in **Supplementary Fig. 8**) was binned at specific time windows to get an evoked spiking activity matrix, y-axis refers to the number of electrodes, x-axis refers to the time bins, and data point indicates the number of spikes at the specific electrode of specific time bin. The spiking activity matrix was further reshaped to 1D vector $\boldsymbol{x}$ to be fed into the simple regression algorithms we used for decoding. The input data were fed into *Brainoware*, and the activity responses were recorded and separated corresponding to each stimulation.

We used Logistic regression for classification tasks, e.g., speech recognition. Logistic regression is one of the simplest and most commonly used ML algorithms for classification. Logistic regression employs a sigmoid function with coefficients in the linear combination to map the vector of regressors $\boldsymbol{x}$ to a categorical target $\boldsymbol{y}$. The possibility of 1D vector $\boldsymbol{x}$ corresponding to different possible outputs is defined by the weight matrix θ [8]:

$$h_\theta(\boldsymbol{x}) = g(\theta^T \cdot \boldsymbol{x})$$

$$g(\boldsymbol{z}) = \frac{1}{1 + e^{-\boldsymbol{z}}}$$

And a linear regression function was employed for predicting the Hénon map equation. Linear regression is widely used in continuous projection, and it assumes the relationship between the dependent variable (target) $\boldsymbol{y}$ and the vector of regressors $\boldsymbol{x}$ is linear, as:

$$y_i = \beta_0 + \beta_1 x_{i1} + \cdots + \beta_p x_{ip} + \varepsilon_i\ , \quad i = 1, \ldots, n,$$

Where ε is an unobserved random variable representing the noise. We used linear regression for predicting non-linear equations, the binned 1D electrical activity vector ***x*** evoked by input stimulation was fed to the linear regression function and output next value ***y*** of the non-linear equation.

The training of read-out function weights was achieved by the Scikit-learning package in Python, which are commonly used packages for the regression model. For the speech recognition task, training or validation was split with 5 times cross-validation from one epoch training data to obtain the performance. As Hénon map prediction was a contimous time series task, the first 100 data points were used for training, while the following 100 data points were used for validation.

Regression score. The regression score was calculated as follows:

$$R^2 = (1 - \frac{\sum_{i=1}^{N}(x_{pred_i} - x_{truth_i})^2}{\sum_{i=1}^{N}(x_{truth_i} - x_{truth_{mean}})^2}$$

Live imaging of organoids and track network. The organoids were transduced with pAAV-hSyn-mCherry (Addgene # 114472-AAV9) to label neurons with mCherry. Each organoid was first infected with virus at 5 μL of 1 × 10^{13} vg/mL pAAV-hSyn-mCherry 100 μL COM overnight, and more medium was added the next day. The organoids were further cultured for 5 days to enable the mCherry expression by neurons. Then the organoids were transferred to a glass-bottom well plate and incubated with 4 μM Cal-520 AM (ab171868) for 2 hours prior to the imaging. A spinning disk confocal microscope was employed to track the neuron changes as well as calcium levels. The calcium levels were measured using a 20x objective lens with 10 FPS over 2 minutes, and the neuron morphology was imaged using a 60x objective lens. Calcium imaging data was analyzed using Suite2p[9] to obtain the spiking activity of each neuron. The connectivity between neurons was then analyzed using the STTC method described above.

Statistical analysis. Statistical analysis was carried out using GraphPad Prism 8. Two sample groups were compared using the students' t-test. Statistical significance was denoted as: *p<0.05, **p<0.01, ***p<0.005. ****p<0.001. Due to the exploratory nature of our experiments, we did not use statistical methods to pre-determine sample sizes, but our sample sizes are similar to the previous reports[5, 10, 11] in brain organoids field.

Supplementary Discussions

Functional maturation of organoids. The functional maturation of organoids was characterized by their development (**Supplementary Fig. 2**) and neural activity (**Supplementary Fig. 3**). The cell identities of the developing organoids were characterized using immunostaining. In response to the progressive culture and induction, the organoids increased in size and showed neuroepithelium-like structures (**Supplementary Fig. 2a**). At the beginning of neural maturation (1 month), the neural progenitor cells (or NPC; SOX2 and PAX6) were characterized to form polarized neuroepithelium-like structures. Progressively, more mature neurons (MAP2) emerged surrounding NPC layers (**Supplementary Fig. 2b**), and the organoids ultimately developed into

concentric multilayer structures consisting of NPCs, intermediate progenitors (TBR2), radial glial cells (HOPX), cortical layer neurons (CTIP2), and Astrocytes (GFAP) (**Supplementary Fig. 2c**). As the neurons matured further, they showed dendritic structures, synaptic ultrastructure, and formed a complex 3D neuronal network (**Supplementary Fig. 4**).

The neural activity of the organoids was recorded to demonstrate the functional maturation of organoids. The cortical organoids at different developmental stages (e.g., 30, 45, 60 days) were plated onto the HD-MEA chips for activity scans (**Supplementary Fig. 3a**). The activity scan result showed a neural activity map corresponding to the physical organoid shape (**Supplementary Fig. 3b,c**). By measuring and analyzing the population of spontaneous neural activity, the organoids were identified to gradually increase electrical activity (quantified by mean firing rate, burst frequency, and synchrony) (**Supplementary Fig. 3d**), indicating a continually developing neural network. Although spontaneous electrical activity was relatively low, it showed overall synchronicity (bursting observed and increased with increased organoid age) and could be evoked by electrical stimuli. As the organoids gradually matured, the network displayed a robust pattern of activity, switching between long periods of quiescence and short bursts of spontaneous network-synchronized spiking (network bursting) (**Supplementary Fig. 3e**). The network bursts first emerged at 30 days but at this age they were infrequent, roughly around every 30 seconds and decayed monotonically to baseline after onset. After another 30-days, the organoids showed a nested and faster oscillatory pattern, indicating the functional maturation of neurons.

Biological response to electrical stimulation. The organoids response to electrical stimulation were studied using live cell imaging, connectivity analysis, immunostaining, and RNA-seq. The neurons within the organoids were labeled with mCherry via adenovirus infection (AAV-hSyn-mCherry). The transduced organoids were incubated with a Calcium dye (Cal520, AAT Bioquest) to monitor the neuronal calcium activity and track functional connectivity changes. The morphology changes of the neuron (e.g., changes of existing dendrites, and emergence of new dendrites) were identified before and after electrical stimulation (**Supplementary Fig. 4a**). Meanwhile, the corresponding changes of the functional connectivity map were obtained via calcium imaging (**Supplementary Fig. 4b**). We found that the changes in the functional connectivity map before/after the electrical stimulation overlapped with the biological neuron morphology changes with the same trend and direction, indicating the electrical stimulation induced changes in neuron morphology, and further reshaped the functional connectivity of the organoid.

To further characterize the electrical stimulation induced biological response, the dendrite spines within the organoids with or without electrical stimulation were stained using PSD95 (post-synaptic marker) and MAP2 (markers of neurons and their dendrites). The stimulated organoids showed significantly more PSD95+ puncta surrounding the neurons than the naïve organoids (**Supplementary Fig. 4c, d**), indicating that electrical stimulation promoted neural connections within the organoids.

Unsupervised learning via the reshaping of functional connectivity. To ensure that the computing and learning of the whole system was conducted by *Brainoware*, we employed simple

read-out functions, logistic regression for classification tasks (audio recognition) and linear regression for regression tasks (Henón map equation). The performance of these two simple functions relied on sample size, and they would not perform better under repeated training with the same dataset. During our training process, we present the same dataset to the *Brainoware* system each time, and the read-out function would not perform significantly differently trained with same data size. Furthermore, we designed several control experiments to validate the learning of *Brainoware* network. We tested HD-MEA without organoids, untrained naïve organoids, organoids treated with K252a (inhibitor of CaM kinase II and phosphorylase kinase, which blocks Ca^{2+} related learning and memory). We found that the HD-MEA without organoids could not compute and learn, and the performance was significantly lower than other groups with organoids, indicating the computing role of organoid network. Finally, organoids treated with K252a showed similar performance to untrained naïve organoids even after 4 rounds of training, which is significantly lower than the trained organoids, indicating the learning achieved by the network organoid requires CaM kinase and is likely mediated by synaptic plasticity.

***Brainoware* vs ANN.** To further demonstrate the performance of *Brainoware*, we compared *Brainoware* with a widely used artificial neural network (ANN) without or with long short-term memory unit, as well as a standard reservoir computing algorithm: Echo state network (ESN) for predicting the Hénon map problem. The two ANNs had three hidden layers (64, 32, 16 neurons), and were trained using the same dataset (total 200 data points, first 100 for training, and the remaining 100 for testing) with adam optimizer for a maximum of 50 epochs. The ESN was implemented using PyRCN[12] to have 32 nodes corresponding to 32 read-out channels of *Brainoware*. As shown in **Supplementary Fig. 11a**, *Brainoware* learnt significantly faster than ANNs and showed higher performance gain under 4 epochs training (Accuracy increase 0.297 for *Brainoware*, 0.034 for ANN w/o LSTM, and 0.041 for ANN w LSTM). Compared with the theoretical output (ground truth, black), *Brainoware* (red) showed better-predicted results than linear regression (blue) and ANN w/o LSTM (green), while ANN w LSTM (gray) and ESN (purple) outperformed *Brainoware* (**Supplementary Fig. 11b, c**).

Supplementary Figures

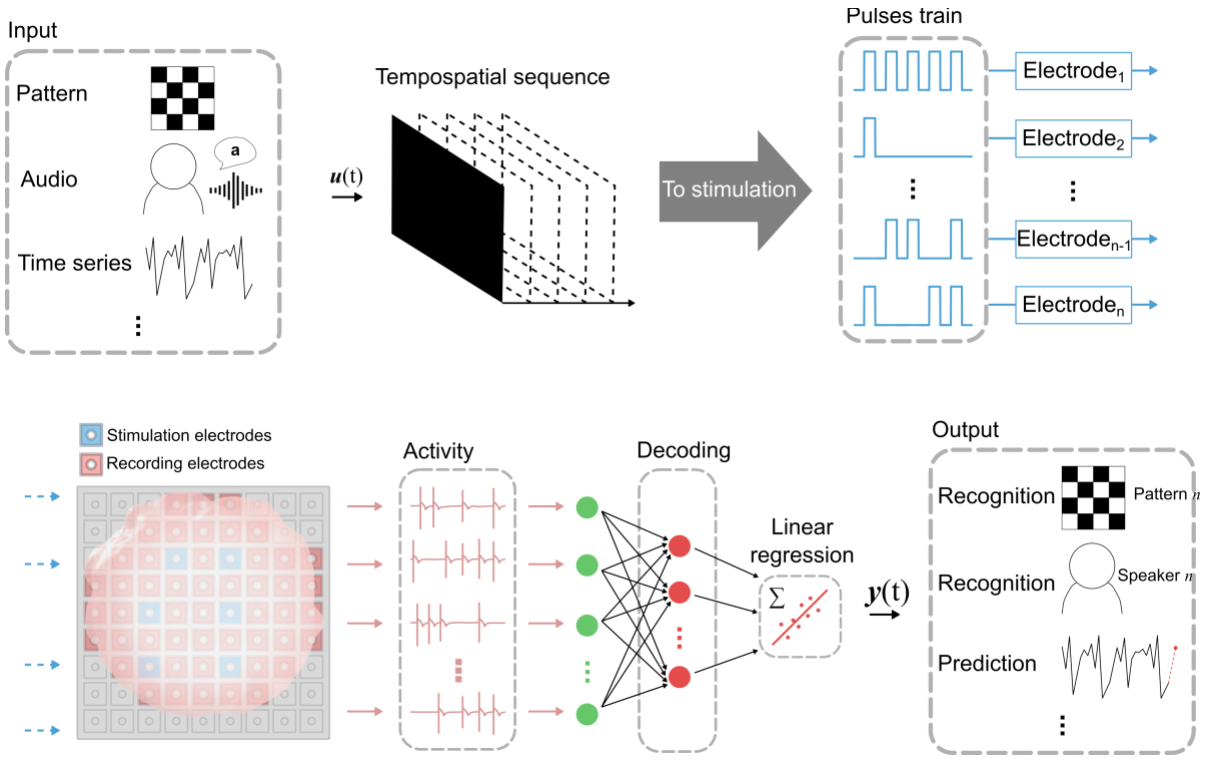

Supplementary Fig. 1. Workflow of *Brainoware* computing. Input information (image pattern, audio clips, time series, etc.) was first converted to a spatiotemporal pattern sequence, and then mapped to stimulation pulse trains applied to stimulation electrodes in the MEA system. The brain organoid receives the input stimulation (**u**(t)), and the evoked neuron activities are recorded by the MEA system and analyzed by a decoding function (linear regression or logistic regression) to output **y**(t) (classification, recognition, prediction, etc.).

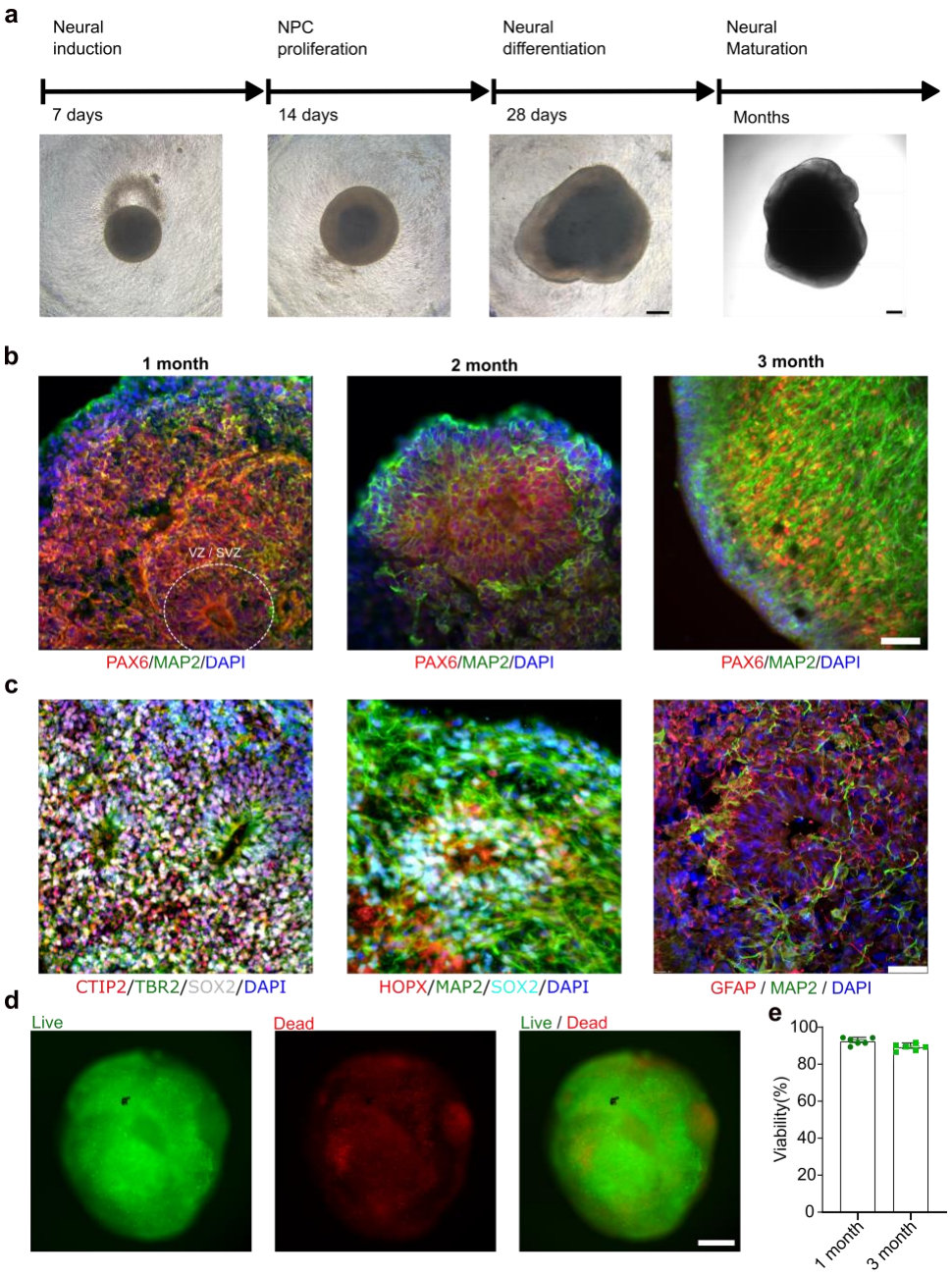

Supplementary Fig. 2. Generation and characterization of human cortical organoids. (**a**) Overview of the protocol used to generate cortical organoids and representative images of cortical organoids at different time stages (Scale bar, 200 μm). (**b**) Representative immunostainings showing the neural maturation of cortical organoids over time (neural progenitor cells, PAX6; mature neurons, MAP2). Scale bar, 20 μm. (**c**) Representative immunostainings showing the basal Radial Glia (RG) progenitor cells (SOX2), intermediate progenitor cells (TBR2), outer radial glial cells (HOPX), cortical layer neurons (CTIP2), astrocytes (GFAP), and neurons over time (Scale bars, 20 μm). (**d**) Representative live/dead staining results of a 3-month human cortical organoids (Scale bars, 200 μm). (**e**) Quantification results of viability in 1-month and 3-month human cortical organoids. (mean ± s.e.m., n = 6 organoids)

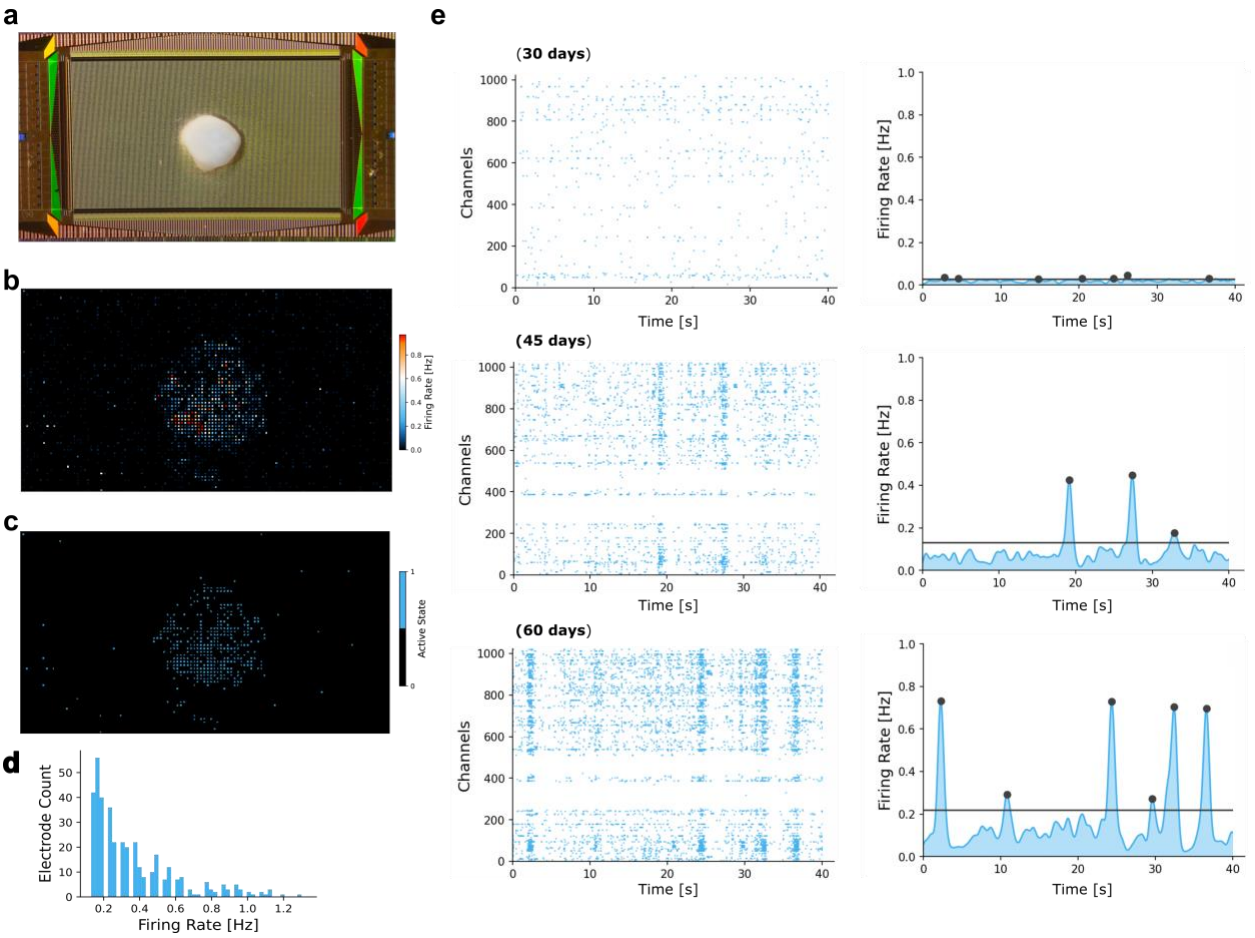

Supplementary Fig. 3. Cortical organoids plating on MEA. (**a**) A representative image of the cortical organoids plated onto a HD-MEA. (**b**) Corresponding representative scanned neuron activities (firing rate) of the plated organoid. The color scale indicates the normalized number of detected spikes (above 5x-rms noise) registered at each electrode site measured over a 30 s interval. (**c**) Representative active electrodes of the plated cortical organoid. (**d**) Representative firing rate distribution of the plated organoid. (**e**) Raster plots and corresponding firing rate plots showing the functional maturation of the representative cortical organoid at 30, 45, and 60 days. The cortical organoid showed network bursting after 45 days culture.

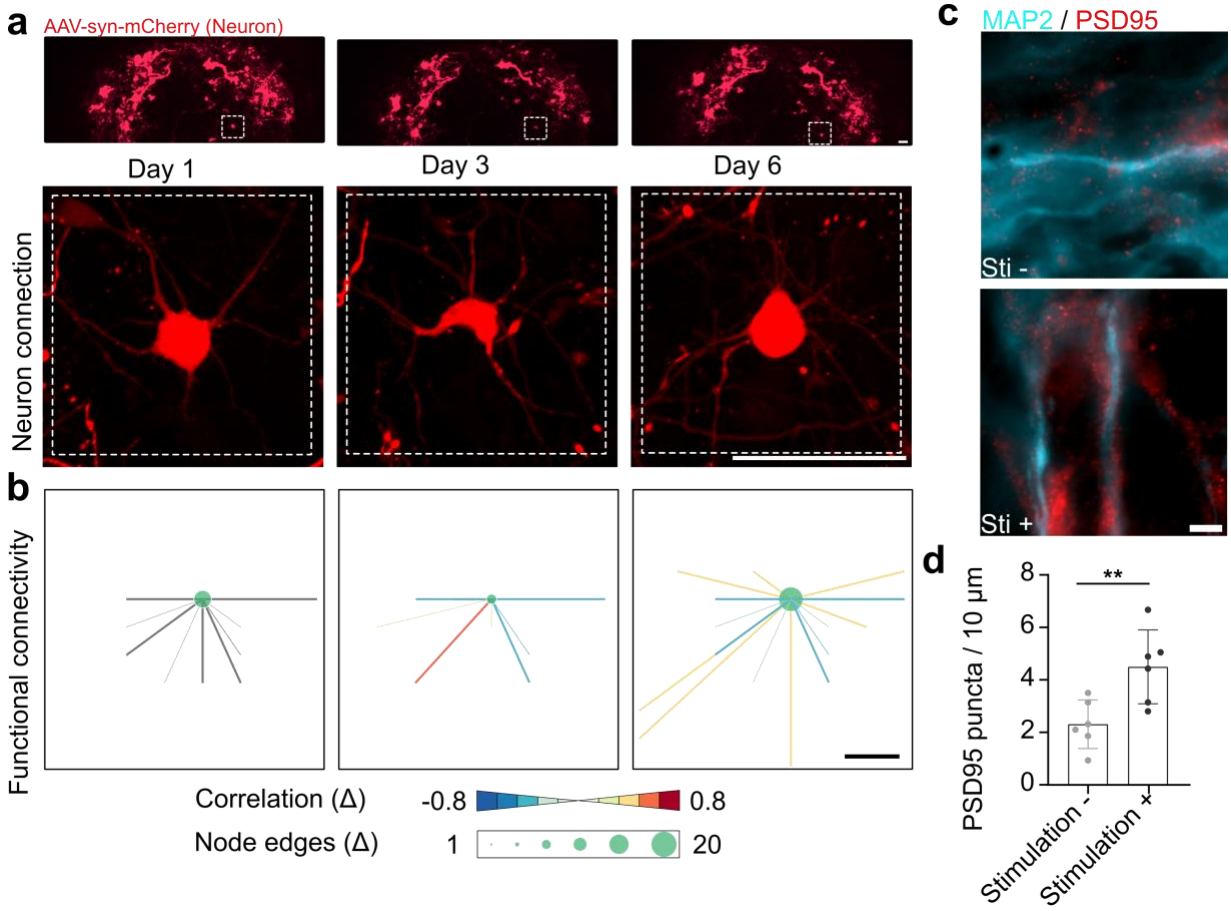

Supplementary Fig. 4. Training reshaped organoid neural networks. (**a**) Reshaping of neuronal morphology during the Hénon map training process (Scale bar, 20 µm). The neurons transfected with AAV-Syn-mCherry are in red, and the bottom image is a zoom (high magnitude image) of the selected region (dashed rectangle) of the top images. (**b**) Corresponding functional connectivity changes to the reshaping of the same neuron in ONNs within the same organoid in (a) during the same training. The functional connectivity is analyzed from Calcium imaging. (**c**) Immunofluorescence staining showing dendritic spines (MAP2, neurons and their dendrites; PSD95, spines) within the organoids after electrical stimulation (Sti+) or the naïve organoids (Sti-) (Scale bar, 20 µm). (**d**) Quantification of PSD95+punti colocalized with Map2 process of the two groups with (stimulation +) or without (stimulation -) electrical stimulation (mean ± s.e.m.,14 areas from 6 organoids from 3 independent experiments, unpaired t test, **p=0.0097).

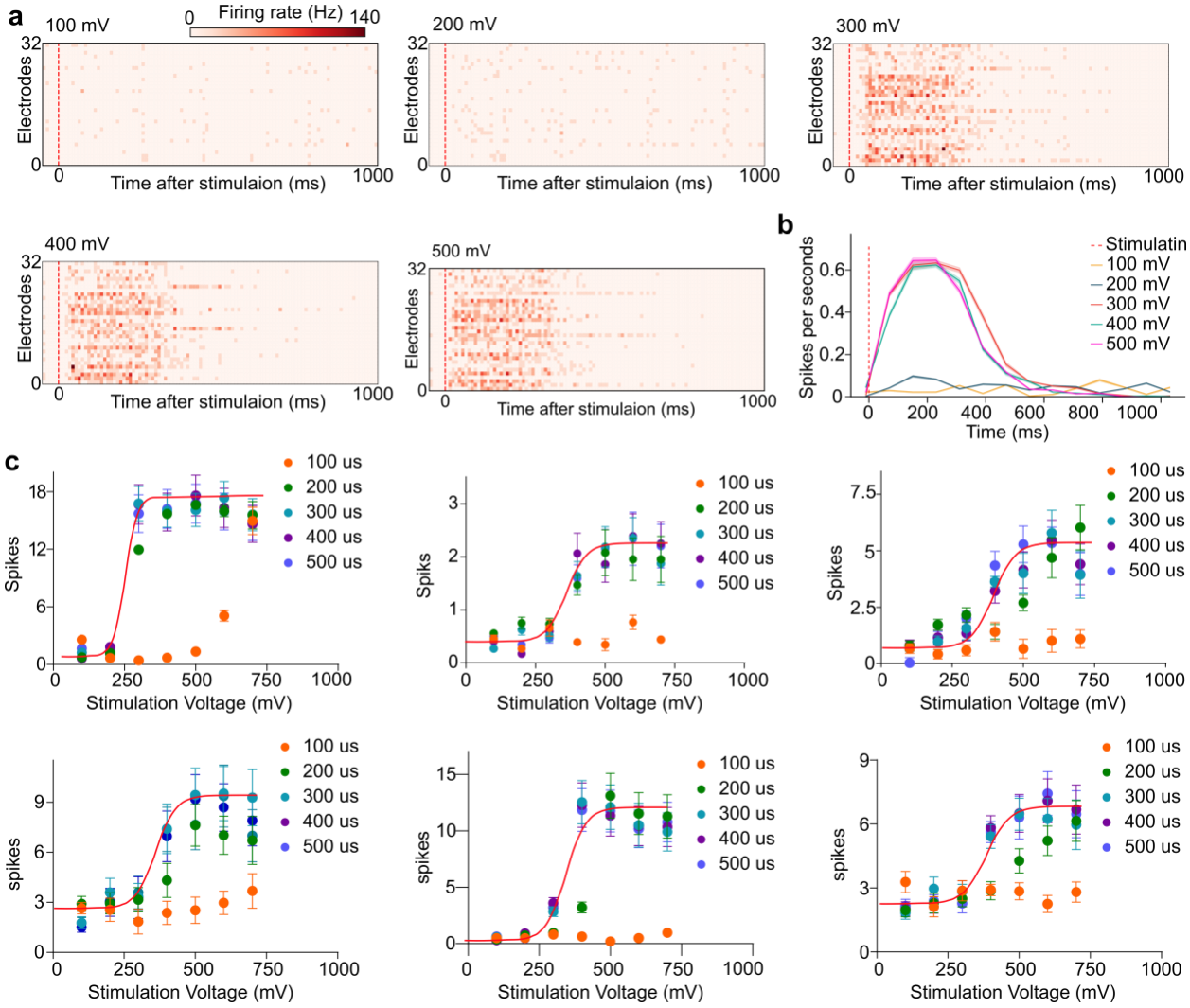

Supplementary Fig. 5. Nonlinear dynamics. (**a**) Raster plot of neuron activities of the top 32 most active electrodes evoked by bipolar electrical stimulation with different amplitudes (300 μs width, 100 mV, 200 mV, 300 mV, 400 mV, 500 mV amplitude) (**b**) Post stimulation histogram of the evoked neuron activities by the five different bipolar electrical stimulation. Stimulation below 300 mV did not evoke a neural activity response, while higher amplitude induced similar responses. (mean ± s.e.m., n = 5 stimulation trials) (**c**) Nonlinear dynamics of 6 different cortical organoids. Symbols with error bars show the experimental evoked neuron activities after a 200 ms duration pulse train with different stimulation voltages and pulse width. The smooth red line is a sigmoid function (one of the most widely used nonlinear activation functions in AI algorithms) fitted on the experiment results. (mean ± s.e.m., n = 5 stimulation trials)

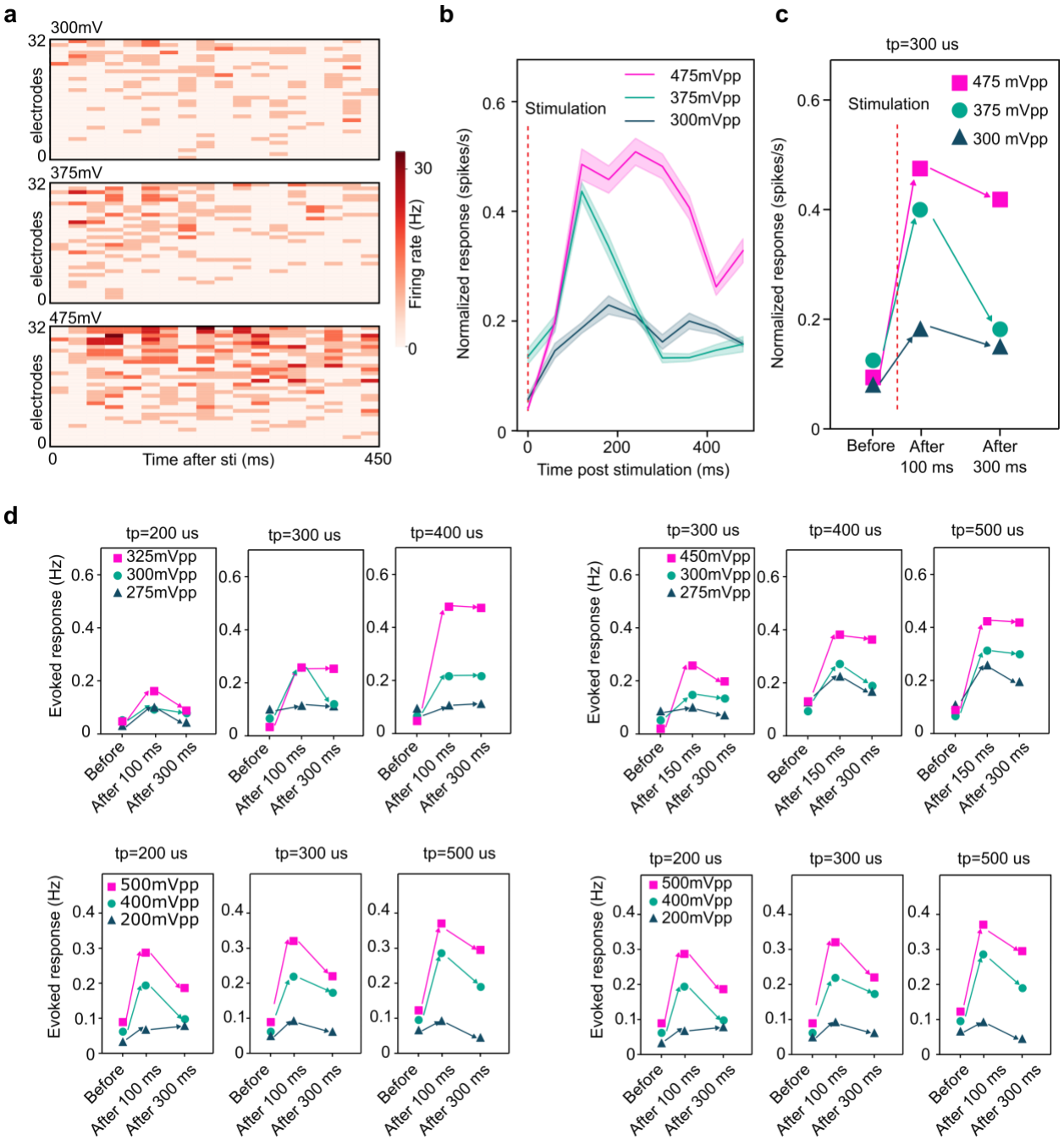

Supplementary Fig. 6. Fading memory. (**a**) Raster plot of neuron activities of the top 32 most active electrodes evoked by bipolar electrical stimulation with different amplitudes (300 μs width, 300 mV, 375 mV, 475 mV amplitude) (**b**) Post stimulation histogram of the evoked neuron activities by the three different bipolar electrical stimulations. Stimulation evoked activities persisted in the brain organoids for a short period of time and gradually fade away. A stronger stimulation evoked longer lasting neural activity responses. (mean ± s.e.m., n = 5 stimulation trials) (**c**) Changes in neuron firing rate in brain organoids 100 and 300 ms after a single pulse stimulus, extracted from (**b**). (**d**) The fading memory property of 4 representative cortical organoids.

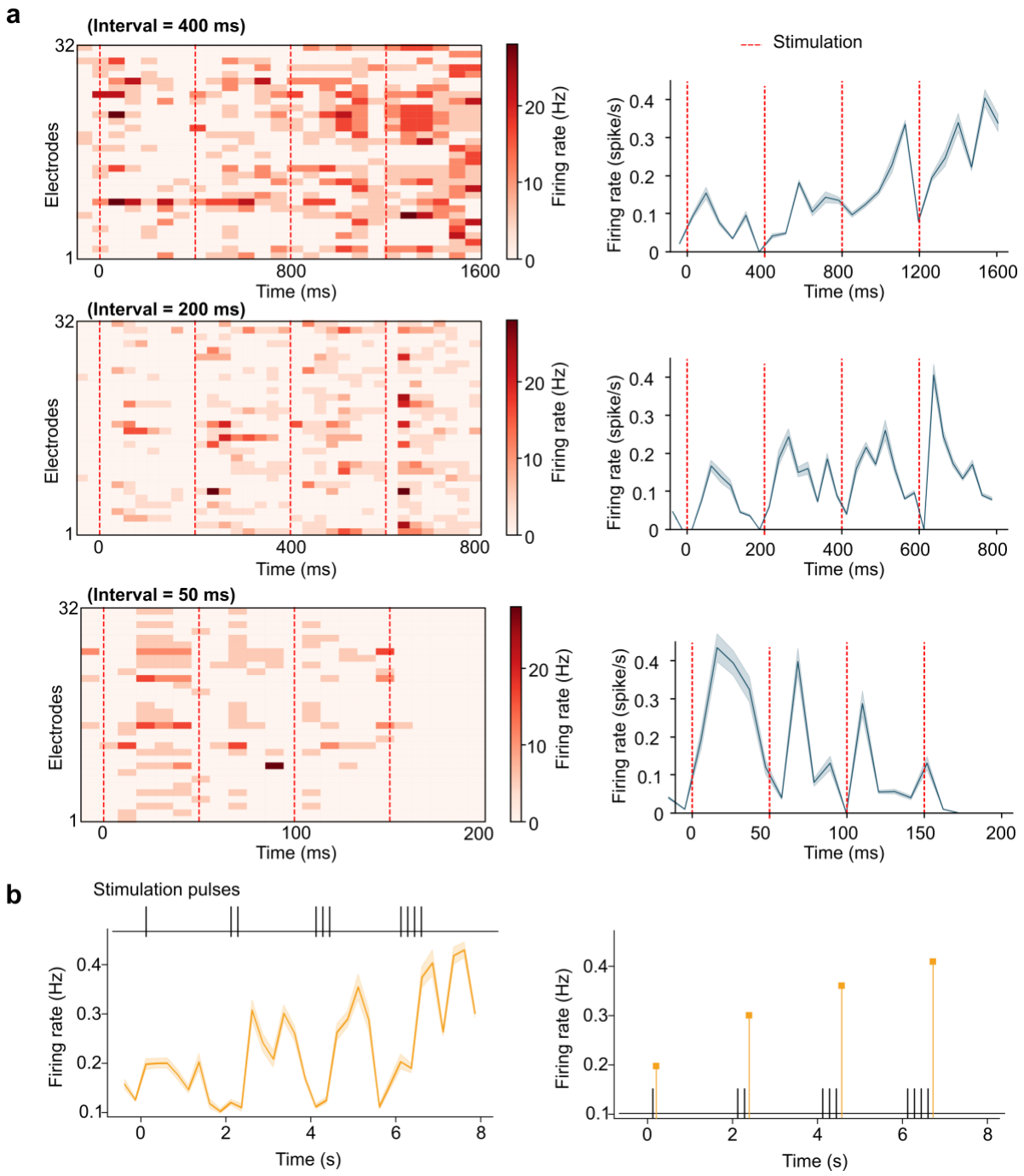

Supplementary Fig. 7. Recurrent effects. (**a**) Stimuli repeating at 400 and 200 ms) induced successively higher responses. In contrast, stimuli repeating 50 ms produced diminishing responses. The minimal stimulation interval was set to 100ms. (mean ± s.e.m., n = 5 stimulation trials) (**b**) Post stimulation histogram of a typical brain organoid to a pulse stream with an increasing number of pulses(left). Extracted organoid's response to varying temporal inputs, like the widely used memristor and neuromorphic AI hardware (right). (mean ± s.e.m., n = 5 stimulation trials, Corresponding to **Fig. 2d**)

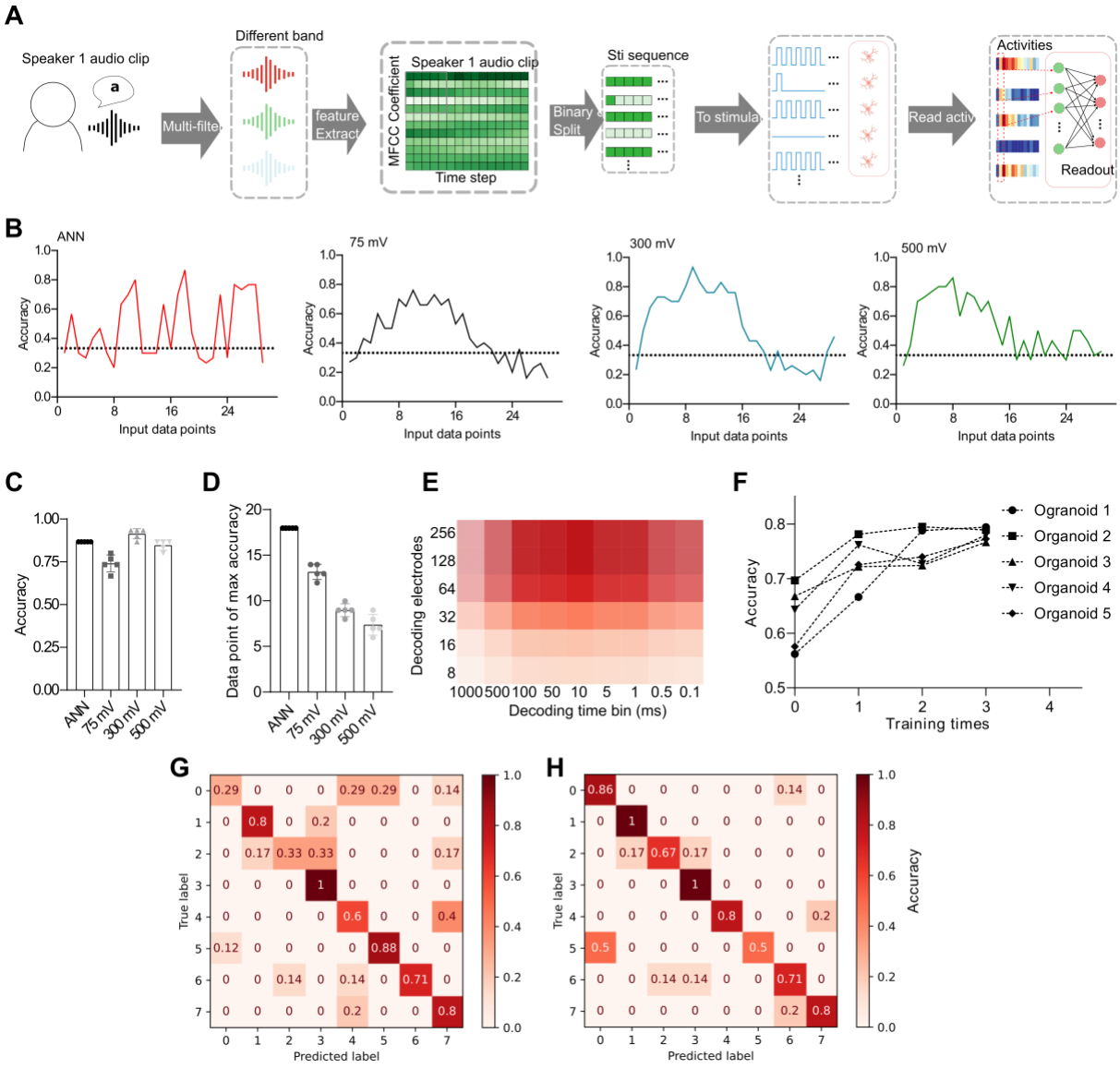

Supplementary Fig. 8. Speech recognition. (**a**) Workflow for speech recognition. (**b**) Recognition accuracy of the first three speakers from the Japanese vowel dataset using ANN without memory, organoids with 75 mV, 300 mV, and 500 mV stimulation over discrete data points. The organoids showed a smoother curve, indicating short-term memory. (**c, d**) Maximum recognition accuracy and the number of data points needed for maximal accuracy for each of the four groups. While all four approaches yield similar accuracy (**c**), *Brainoware* requires fewer data point inputs to reach maximum accuracy (mean ± s.e.m., n=5, 3 independent experiments). (**e**) Optimization of the decoding parameters. 64 electrodes, 10ms gave us the best results. (**f**) Learning curve of individual organoids (mean ± s.e.m., n=5, 3 independent experiments) on the whole dataset, classification accuracy plateaued by the third training session. (**g, h**) Representative confusion matrix with detailed ratio labeled of organoids before and after training. (Corresponding to **Fig. 3c**)

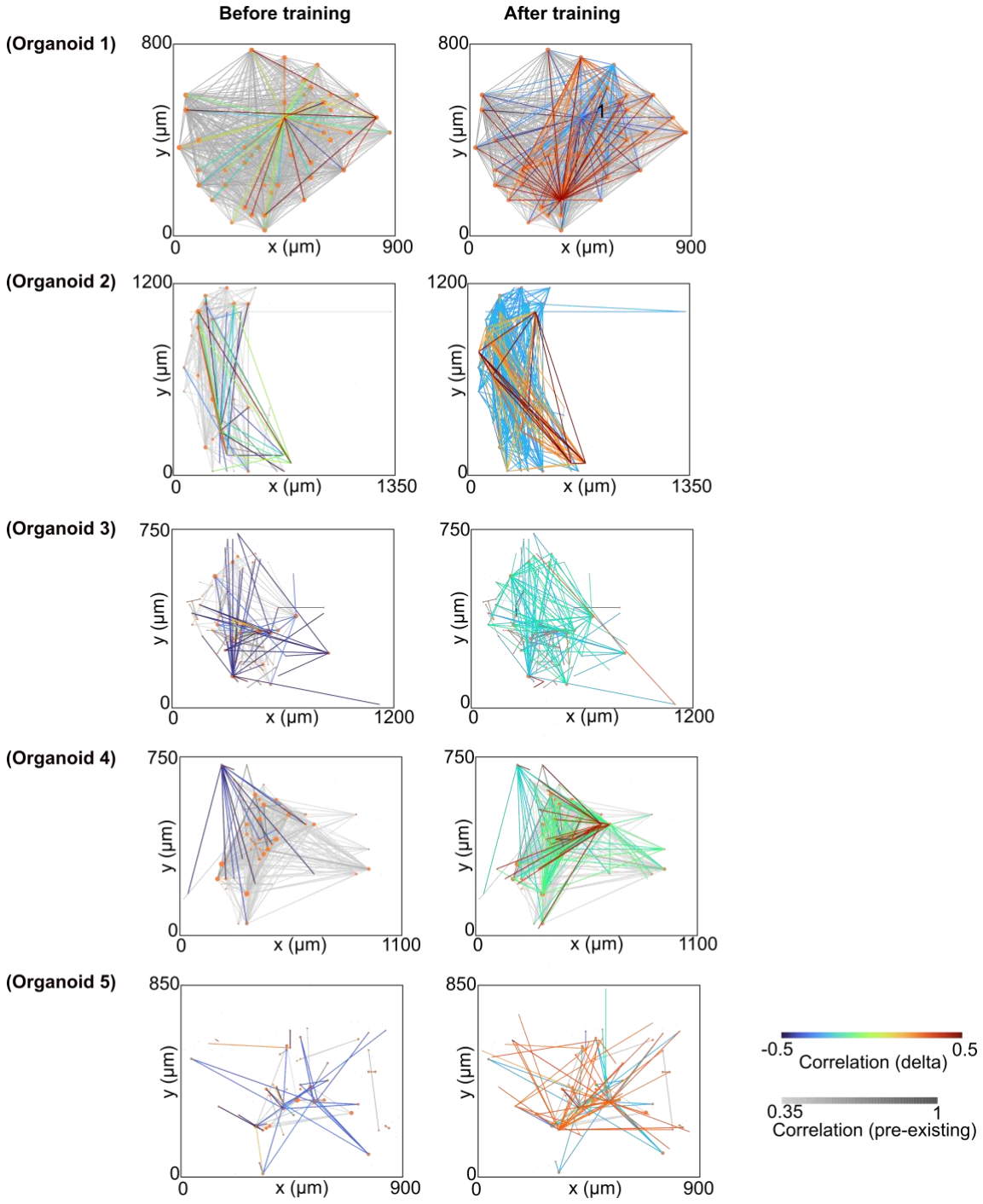

Supplementary Fig. 9. Functional connectivity before/after training. The functional connectivity of 5 different organoids before and after training.

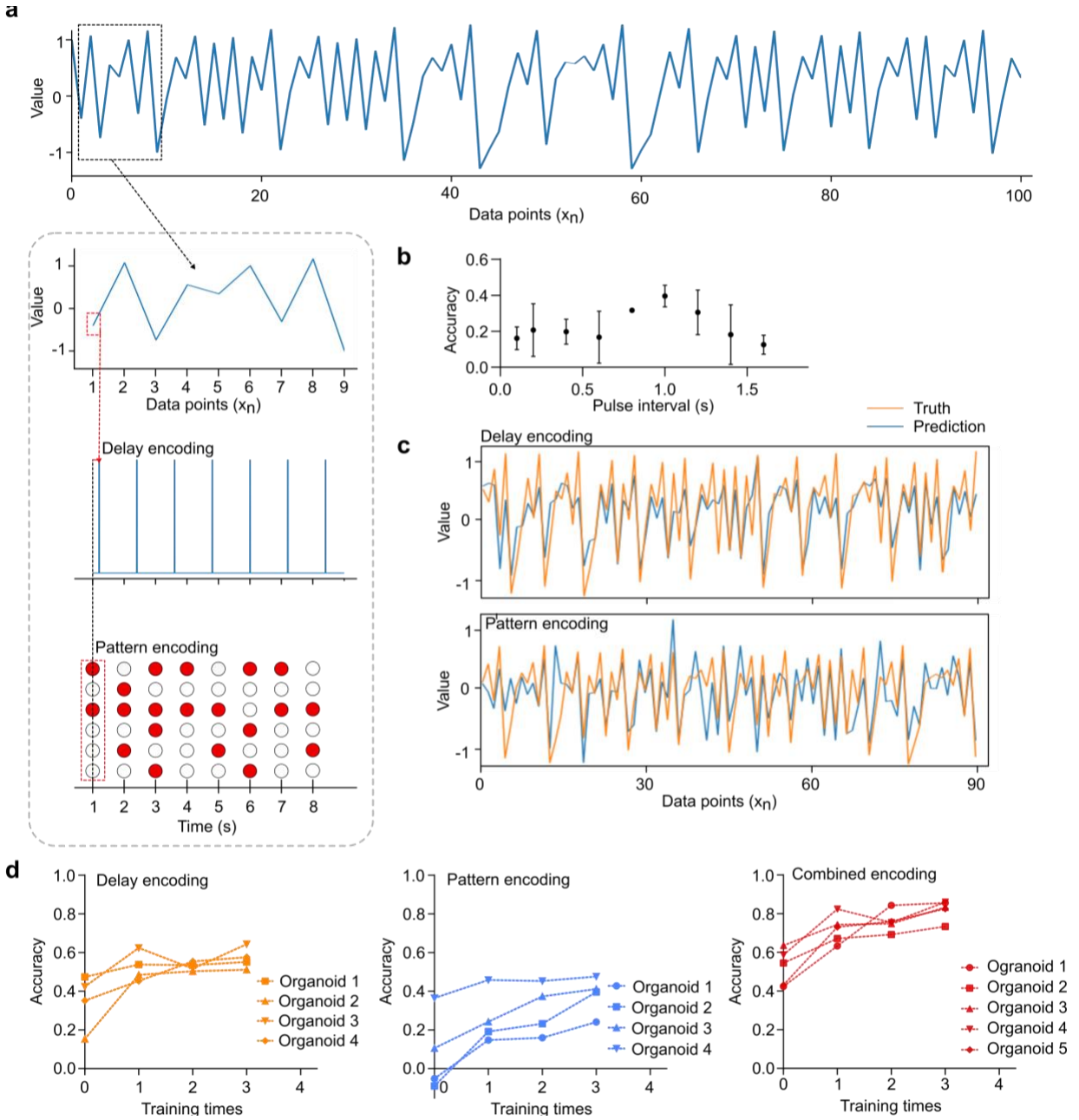

Supplementary Fig. 10. Predicting the Hénon map via different encoding methods (spatial or temporal or combination). (**a**) Hénon map data are encoded into electrical stimulation pulse train via latency encoding (temporal) and patterned electrical stimulation via pattern encoding (spatial). (**b**) Optimization of stimulation interval for predicting the Hénon map equation. A 1s interval shows the best outcome. (mean ± std, n = 3 organoids) (**c**) The predicted results obtained by the living computing system via temporal and spatial encoding, where the orange line represents the ideal target, and the blue line represents the experimental output from the living computing system. (**d**) Learning curves of 4 individual organoids on delay, pattern, and combined (delay + pattern) encoding method. The combined encoding strategy could provide the optimal performance for the on-chip learning of Brainoware.

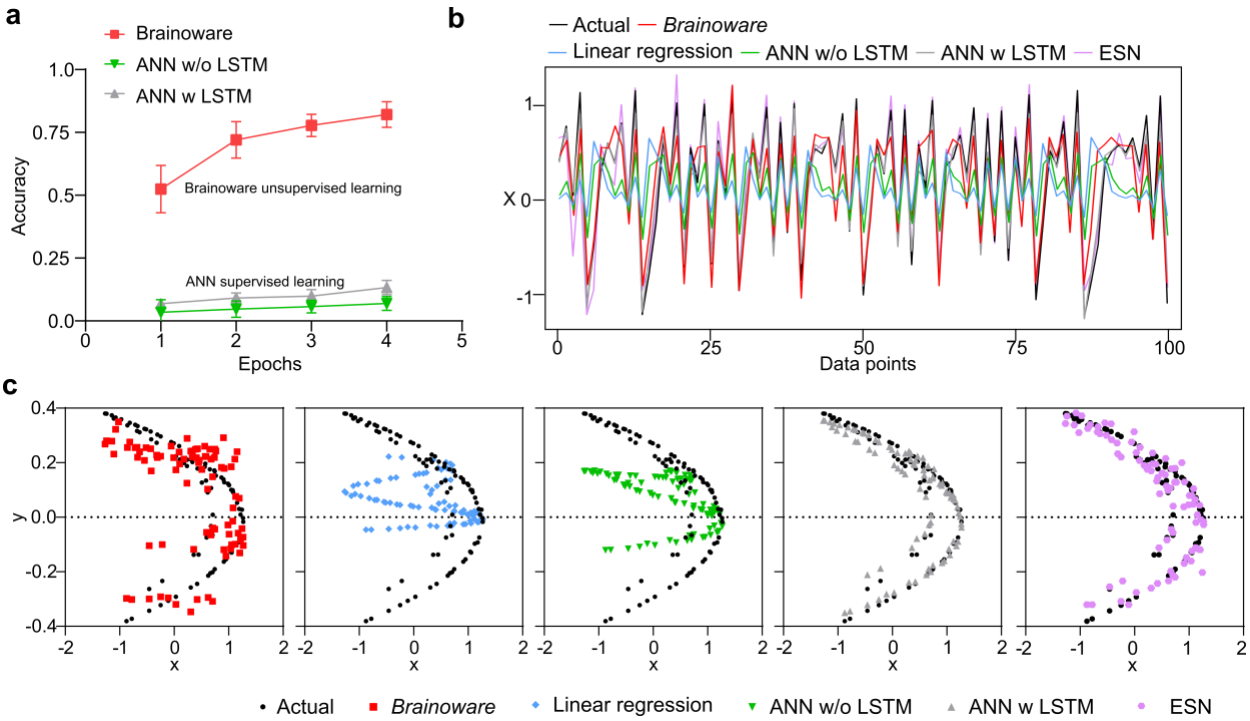

Supplementary Fig. 11. Comparison of Brainoware with an artificial neural network (ANN) with or without a long short-term memory (LSTM) unit and echo state network (ESN, a standard reservoir computing algorithm) on predicting the Hénon map. (**a**) Learning curves of *Brainoware* unsupervised learning, ANN w/o LSTM, and ANN w LSTM supervised learning over training epochs. (mean ± s.e.m., n=5, 3 independent experiments) (**b**) Predicted X values using *Brainoware* (4 epochs), ANN w/o LSTM (50 epochs), ANN w LSTM (50 epochs), and ESN vs ground true X value. (**c**) Predicted 2D maps using *Brainoware* (4 epochs), linear regression, ANN w/o LSTM (50 epochs), ANN w LSTM (50 epochs), and ESN vs ground true 2D map.

Supplementary Tables

	Neuromorphic chips	**2D conventional neuron cultures**	**Brain organoids**	**Human brains**
Size	10^2 to 10^4 nodes[13]	1,800-2,000 cells / mm^2 [14]	10^6 to 10^7 of cells[15] per organoid	10^{11} neurons[16]
Complexity	2D silicon chips	Most 2D network	3D network with various cells like an immature brain[17]	A huge 3D network with mature cell types for different functions[16]
Connections	2D connections[16]	Connections largely limited to side-by-side contact[18]	3D connections with complex network[5, 18]	3D connections with small world property[19]
Learning	Partially mimicking synapse[16]	Limited neurogenesis and partial neuron plasticity (2D environment)[20]	Partial neuron plasticity and neurogenesis[17]	Full neuron plasticity and neurogenesis[16]

Table 1. Comparison of neuromorphic chips, 2D neurons, brain organoids, and human brains.

Cortical Organoid Medium 1: EB Formation Medium	**Day 0**
COMPONENTS	**CONCENTRATION**
mTeSR1	1X
SB431542	10 µM
XAV939	2 µM
Dorsomorphin	1 µM
Y-27632 **(only for 24h)**	90 µM
Cortical Organoid Medium 2 - Proliferation Medium	**Day 3**
COMPONENTS	**CONCENTRATION**
Neuralbasal	1X
GlutaMax (100X)	1X
Gem21 (50X)	1X
N2 NeuroPlex (100X)	1X
MEM-NEAA (100X)	1X
Penn/Strep (100X)	1X

SB-431542	10 µM
XAV939	2 µM
Dorsomorphin	1 µM
Cortical Organoid Medium 3- Expansion Medium	**Day 10**
COMPONENTS	**CONCENTRATION**
Neuralbasal	1X
GlutaMax (100X)	1X
Gem21 (50X)	1X
N2 NeuroPlex (100X)	1X
MEM-NEAA (100X)	1X
Penn/Strep (100X)	1X
FGF-2	20 ng/mL
Cortical Organoid Medium 4 - Differentiation Medium	**Day 17**
COMPONENTS	**CONCENTRATION**
Neuralbasal	1X
GlutaMax (100X)	1X
Gem21 (50X)	1X
N2 NeuroPlex (100X)	1X
MEM-NEAA (100X)	1X
Penn/Strep (100X)	1X
FGF-2	20 ng/mL
EGF	20 ng/mL
Cortical Organoid Medium 5 - Maturation Medium	**Day 24**
COMPONENTS	**CONCENTRATION**
Neuralbasal	1X
GlutaMax (100X)	1X
Gem21 (50X)	1X
N2 NeuroPlex (100X)	1X
MEM-NEAA (100X)	1X
Penn/Strep (100X)	1X
BDNF (100µg/mL)	10 ng/mL
GDNF (10mg/mL)	10 ng/mL
NT3 (100µg/mL)	10 ng/mL

Ascorbic Acid	200 µM
dibutyryl-cAMP	1000 µM
Cortical Organoid Medium 6 - Maintenance Medium	**Day 31**
COMPONENTS	**CONCENTRATION**
Neuralbasal	1X
GlutaMax (100X)	1X
Gem21 (50X)	1X
N2 NeuroPlex (100X)	1X
MEM-NEAA (100X)	1X
Penn/Strep (100X)	1X
Cortical Organoid Medium 7 - BrainPhys Medium	**Day 45**
COMPONENTS	**CONCENTRATION**
Brainphys Imaging Optimized Medium	1X
NeuroCult SM1 supplement	1X
GlutaMax (100X)	1X
cAMP (10mM)	100 µM
Penn/Strep (100X)	1X

Table 2. Medium composition for organoids.

Marker	Host	Vendor	Catalot#	Dilution
CTIP2	Rat	Abcam	AB18465	1:500
TBR2	Chicken	Millipore	AB15894	1:200
SOX2	Goat	R&D	AF2018-SP	1:500
PAX6	Rabbit	BioLegend	901301	1:200
GFAP	Rabbit	Abcam	ab7260	1:500
MAP2	Chicken	Millipore	AB5543	1:500
PSD-95	Rabbit	Cell Signaling	3450S	1:200
HOPX	Rabbit	Sigma	HPA030180	1:200
Tuj1	Rabbit	Cell Signaling	D71G9	1:500
Alexa 488-Chicken	Donkey	Jackson	703-545-155	1:200
Alexa 488-Rat	Donkey	Life technologies	A21208	1:500
Alexa 488-Goat	Donkey	Jackson	705-545-003	1:200
Alexa 594-Rabbit	Donkey	Life technologies	A21207	1:500
Alexa 647-Goat	Donkey	Life technologies	A21447	1:500

Table 3. Antibody information and dilution factors.

Supplementary References

1. Pachitariu, M., Steinmetz, N., Kadir, S., Carandini, M. & D., H.K. Kilosort: realtime spike-sorting for extracellular electrophysiology with hundreds of channels. *bioRxiv*, 061481 (2016).
2. Buccino, A.P. et al. SpikeInterface, a unified framework for spike sorting. *Elife* **9**, e61834 (2020).
3. Cutts, C.S. & Eglen, S.J. Detecting Pairwise Correlations in Spike Trains: An Objective Comparison of Methods and Application to the Study of Retinal Waves. *The Journal of Neuroscience* **34**, 14288-14303 (2014).
4. Denker, M., Yegenoglu, A. & Grün, S. (Computational and Systems Neuroscience, 2018).
5. Sharf, T. et al. Functional neuronal circuitry and oscillatory dynamics in human brain organoids. *Nature Communications* **13**, 4403 (2022).
6. Sahidullah, M. & Saha, G. Design, analysis and experimental evaluation of block based transformation in MFCC computation for speaker recognition. *Speech communication* **54**, 543-565 (2012).
7. Zheng, F., Zhang, G. & Song, Z. Comparison of different implementations of MFCC. *Journal of Computer Science and Technology* **16**, 582-589 (2001).
8. Bishop, C.M. & Nasrabadi, N.M. Pattern recognition and machine learning, Vol. 4. (Springer, 2006).
9. Pachitariu, M. et al. (bioRxiv, 2016).
10. Trujillo, C.A. et al. Complex Oscillatory Waves Emerging from Cortical Organoids Model Early Human Brain Network Development. *Cell Stem Cell* **25**, 558-569.e557 (2019).
11. Giandomenico, S.L. et al. Cerebral organoids at the air–liquid interface generate diverse nerve tracts with functional output. *Nature Neuroscience* **22**, 669-679 (2019).
12. Steiner, P., Jalalvand, A., Stone, S. & Birkholz, P. PyRCN: A toolbox for exploration and application of Reservoir Computing Networks. *Engineering Applications of Artificial Intelligence* **113**, 104964 (2022).
13. Furber, S. Large-scale neuromorphic computing systems. *Journal of Neural Engineering* **13**, 051001 (2016).
14. Frega, M., Tedesco, M., Massobrio, P., Pesce, M. & Martinoia, S. Network dynamics of 3D engineered neuronal cultures: a new experimental model for in-vitro electrophysiology. *Scientific Reports* **4**, 5489 (2014).
15. Trujillo, C.A. & Muotri, A.R. Brain Organoids and the Study of Neurodevelopment. *Trends in Molecular Medicine* **24**, 982-990 (2018).
16. Marković, D., Mizrahi, A., Querlioz, D. & Grollier, J. Physics for neuromorphic computing. *Nature Reviews Physics* **2**, 499-510 (2020).
17. Di Lullo, E. & Kriegstein, A.R. The use of brain organoids to investigate neural development and disease. *Nature Reviews Neuroscience* **18**, 573-584 (2017).
18. Centeno, E.G.Z., Cimarosti, H. & Bithell, A. 2D versus 3D human induced pluripotent stem cell-derived cultures for neurodegenerative disease modelling. *Molecular Neurodegeneration* **13**, 27 (2018).
19. Liao, X., Vasilakos, A.V. & He, Y. Small-world human brain networks: Perspectives and challenges. *Neuroscience & Biobehavioral Reviews* **77**, 286-300 (2017).
20. Jensen, C. & Teng, Y. Is It Time to Start Transitioning From 2D to 3D Cell Culture? *Frontiers in Molecular Biosciences* **7** (2020).